ATP-EMTP investigation of a new algorithm for locating faults on power transmission lines with use of two-end unsynchronized measurements

M. M. Saha, J. Izykowski, E. Rosolowski, R. Molag

Abstract--This paper presents an algorithm for locating faults on two-terminal power transmission lines. Unsynchronized two-end voltages and currents are processed in the algorithm for determining the distance to fault and the synchronization angle. The calculations are performed initially for the lumped model of the transmission line. Then, these results are used as the initial data for the Newton-Raphson method based iterative calculations, in which the distributed parameter line model is utilized. The delivered fault location algorithm has been tested and evaluated with the fault data obtained from versatile ATP-EMTP simulations of faults in the power network containing the 400 kV, 300 km transmission line. The sample results of the evaluation are reported and discussed.

Keywords: ATP-EMTP, power transmission line, fault simulation, digital measurement, unsynchronized measurements, fault location algorithm.

I. Introduction

Location of faults on overhead power lines for the inspection-repair purpose [1–10] is aimed at accurate pin-pointing of faults, which is required by operators and utility staff in order to expedite service restoration and thus to reduce outage time, operating costs and customer complains. Varieties of fault location algorithms have been developed so far. Majority of them, including the fault location algorithm presented in this paper, is based on an impedance principle, making use of the fundamental frequency voltages and currents. Depending on the availability of the fault locator input signals they can be categorized as:

- one-end algorithms [1]–[2],
- two-end and multi-end algorithms [4]–[10].

One-end impedance-based fault location algorithms [1]–[2] utilize voltages and currents acquired at particular end of the line. Such technique is very simple and is commonly incorporated into the microprocessor-based protective relays.

Two-end algorithms [5]–[10] process signals from both terminals of the line and thus larger amount of information [5]–[10] is utilized. Performance of the two-end algorithms is generally superior in comparison to the one-end approaches.

Digital measurements at different line terminals can be performed synchronously if the GPS (Global Positioning System) [3] is available. This allows performing simple and accurate fault location [5]. This paper considers the case of two-end unsynchronized measurements (Fig. 1 – Fig. 2), for which the A/D converters at the line terminals are not controlled by the GPS.

Fig. 1 presents schematically the considered two-end fault location on two-terminal transmission line AB. The fault locator (FL) is here shown as a stand-alone device, however, it can be also associated with the measurement unit at either side of the line (MU_A or MU_B). At both terminals there are current transformers (CTs_A, CTs_B) and voltage transformers (VTs_A, VTs_B) transforming signals to the measurement units. In these units digital measurements are performed for determining the phasors of currents ($\underline{I}_{A\{a,b,c\}}$, $\underline{I}_{B\{a,b,c\}}$) and voltages ($\underline{V}_{A\{a,b,c\}}$, $\underline{V}_{B\{a,b,c\}}$) from three-phases (a, b, c).

In case of two-end unsynchronized measurements [6]–[10] the sampling instants at the A and B ends (marked in Fig. 2 by small circles) do not coincide due to lack of the GPS control.

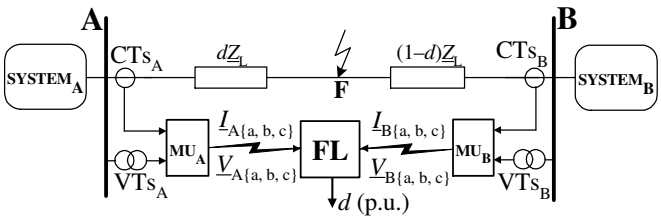

Fig. 1. Schematic diagram for two-end unsynchronized fault location.

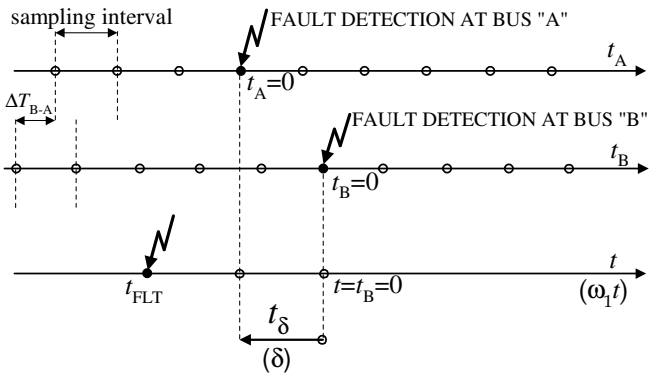

Fig. 2. Need for phase alignment in case of using two-end unsynchronized measurements.

This work was supported in part by the Ministry of Science and Higher Education of Poland under Grant 3 T10B 070 30.

M. M. Saha is with the ABB, Västerås SE-721 59, Sweden (e-mail of corresponding author: murari.saha@se.abb.com).

J. Izykowski, E. Rosolowski, R. Molag are with the Wroclaw University of Technology, Wroclaw 50-370, Poland (e-mail: jan.izykowski@pwr.wroc.pl; eugeniusz.rosolowski@pwr.wroc.pl, rafal.molag@wp.pl).

Presented at the International Conference on Power Systems Transients (IPST'07) in Lyon, France on June 4-7, 2007

As a result of not using the GPS control, a certain random shift ($\Delta T_{B\text{-}A}$) exists between the sampling instants of the both ends. Moreover, the instant at which the fault is detected is usually considered as the time stamp: t_A=0 (at the bus A) and t_B=0 (at the bus B), which also do not coincide. In consequence, the measurements from both ends do not have a common time base. In order to assure such common base one has to take the measurements from the particular end as the base (for example from the terminal B, as it will be assumed in all further considerations), while for the other terminal (the terminal A) needs to introduce the respective alignment. In case of formulating the fault location algorithm in terms of phasors of the measured quantities, phase alignment is done by multiplying all the phasors from the terminal A by the synchronization operator exp(jδ), where: δ – synchronization angle. In general, the unknown synchronization angle δ can be:

- eliminated by mathematical manipulations [9],
- calculated from the pre-fault quantities [4],
- calculated from the fault quantities [6], [8], [10].

This paper presents a fault location algorithm, which calculates a distance to fault by processing unsynchronized two-end measurements of voltages and currents with calculation of the synchronization angle. In order to ensure high accuracy of fault location the distributed parameter line model is strictly taken into account in the presented algorithm.

II. FAULT LOCATION ALGORITHM

The symmetrical components approach appears as very effective technique for transposed lines and, therefore, the fault location algorithm presented here is formulated in terms of these components. In general, the following symmetrical components of the measured quantities can be processed in the algorithm, namely:

- positive sequence components,
- superimposed positive sequence components,
- negative sequence components,
- zero sequence components.

Due to uncertainty with respect to the impedance data of transmission lines for the zero sequence and also presence of mutual coupling of parallel lines for this sequence – in case of double circuit lines, use of the zero sequence voltages and currents is not advantageous. For untransposed lines there is also a possibility for determining the transformation matrix, which can be applied for transforming the coupled phase quantities to decoupled modal quantities with eigenvalue/eigenvector theory [11]. Thus, the presented fault location algorithm is also applicable for untransposed lines.

A. Fault location algorithm – lumped line model

In the initial stage of the presented fault location method, the lumped model of a transmission line with neglecting shunt parameters is considered. The results obtained under such simplification are then used as the starting calculation data for the algorithm formulated further (Section *B*) with use of the distributed parameter line model.

First, the phasors of the symmetrical components (subscripts: 0, 1, 2 standing for the zero-, positive- and negative-sequences) are calculated from three-phase quantities (subscripts: a, b, c denoting the phases). As, for example, in case of the voltages from the terminal A, one determines:

$$\begin{bmatrix} \underline{V}_{A0} \\ \underline{V}_{A1} \\ \underline{V}_{A2} \end{bmatrix} = \frac{1}{3}\begin{bmatrix} 1 & 1 & 1 \\ 1 & \underline{a} & \underline{a}^2 \\ 1 & \underline{a}^2 & \underline{a} \end{bmatrix} \cdot \begin{bmatrix} \underline{V}_{Aa} \\ \underline{V}_{Ab} \\ \underline{V}_{Ac} \end{bmatrix} \tag{1}$$

where: $\underline{a} = \exp(\mathrm{j}2\pi/3)$.

In order to ensure generalization of further considerations, the algorithm is formulated for the *i*-th symmetrical components, where the type (*i*-th) of the components is at choice of the user. One has to take into account the restrictions for using particular symmetrical components [10].

The voltage at the fault point F, viewed from the terminals A and B, is determined as follows:

$$\underline{V}_{FAi}(d,\delta) = \underline{V}_{FAi}^{\text{unsynchr}}\, \mathrm{e}^{\mathrm{j}\delta} \tag{2}$$

$$\underline{V}_{FBi}(d) = \underline{V}_{Bi} - (1-d)\underline{Z}_{iL}\underline{I}_{Bi} \tag{3}$$

where:

$\underline{V}_{FAi}^{\text{unsynchr}}(d) = \underline{V}_{Ai} - d\underline{Z}_{iL}\underline{I}_{Ai}$ – voltage viewed from the terminal A, considered as 'unsynchronized' quantity, what is a consequence of assuming the measurements of the terminal B as the basis,

d – unknown distance to fault from bus A in per unit (p.u.),

$\mathrm{e}^{\mathrm{j}\delta} = \cos(\delta) + \mathrm{j}\sin(\delta)$ – synchronization operator,

$\underline{Z}_{iL}$ – impedance of the line AB for the *i*-th symmetrical component,

$\underline{V}_{Ai}$, $\underline{V}_{Bi}$, $\underline{I}_{Ai}$, $\underline{I}_{Bi}$ – voltage and current phasors from the terminals A and B, respectively, for the *i*-th symmetrical component.

The voltages at the fault point F viewed from both line terminals A and B are identical and thus:

$$\underline{V}_{FAi}(d,\delta) = \underline{V}_{FBi}(d) \tag{4}$$

Substituting (2) and (3) into (4) and then resolving (4) into the real/imaginary parts, with simultaneous elimination of the unknown distance to fault, results in the following compact formula:

$$A_i \cos(\delta_i) + B_i \sin(\delta_i) = C_i \tag{5}$$

where:

$$A_i = \mathrm{imag}\left(\underline{Z}_{iL}^{*}\left((\underline{V}_{Bi} - \underline{Z}_{iL}\underline{I}_{Bi})\underline{I}_{Ai}^{*} - \underline{V}_{Ai}\underline{I}_{Bi}^{*}\right)\right),$$

$$B_i = \mathrm{real}\left(-\underline{Z}_{iL}^{*}\left((\underline{V}_{Bi} - \underline{Z}_{iL}\underline{I}_{Bi})\underline{I}_{Ai}^{*} + \underline{V}_{Ai}\underline{I}_{Bi}^{*}\right)\right),$$

$$C_i = \mathrm{imag}\left(-\underline{Z}_{iL}^{*}\left((\underline{V}_{Bi} - \underline{Z}_{iL}\underline{I}_{Bi})\underline{I}_{Bi}^{*} - \underline{V}_{Ai}\underline{I}_{Ai}^{*}\right)\right),$$

$\underline{x}^{*}$ – conjugate of $\underline{x}$.

In [6], the formula analogous to (5) is solved using Newton-Raphson iterative calculations. The initial guess δ_i=0 has been recommended there for starting these calculations. In order to avoid the iterative calculations at this stage, rewriting (5) to the following form has been proposed:

$$\sin\left(\delta_{i\_1(2)}+\alpha_i\right)=C_i\Big/\sqrt{A_i^{\,2}+B_i^{\,2}} \tag{6}$$

where:

$\sin(\alpha_i)=A_i\Big/\sqrt{A_i^{\,2}+B_i^{\,2}}$, $\cos(\alpha_i)=B_i\Big/\sqrt{A_i^{\,2}+B_i^{\,2}}$.

Two solutions of the trigonometric equation (6) from the range (–π, π) are as follows:

$$\delta_{i\_1}=\operatorname{asin}\left(C_i\Big/\sqrt{A_i^{\,2}+B_i^{\,2}}\right)-\operatorname{atan2}\left(\sin(\alpha_i),\,\cos(\alpha_i)\right) \tag{7}$$

$$\delta_{i\_2}=-\operatorname{asin}\left(C_i\Big/\sqrt{A_i^{\,2}+B_i^{\,2}}\right)-\operatorname{atan2}\left(\sin(\alpha_i),\,\cos(\alpha_i)\right)-\pi \tag{8}$$

where:

atan2 – four quadrant arctangent function for calculating the angle from the sine and cosine values of this angle ('atan2' function is used in Matlab program [12]).

Performing calculations according to (7)–(8) one has:

- to take the real part from the arcsine function since during presence of transient errors the value for the term: $C_i\Big/\sqrt{A_i^{\,2}+B_i^{\,2}}$ could get out from the range (–1, 1),
- to limit the values for the synchronization angle $\delta_{i\_1(2)}$ to the range (–π, π) by adding or subtracting 2π, if happens that the values $\delta_{i\_1(2)}$ get outside the range (–π, π).

Limitation of the synchronization angle to the range (–π, π) is reasonable, since the synchronization angle is a small value [4]. The way of selecting the valid solution is explained further in the relation to the fault location example (Fig. 3 – Fig. 5).

After determination of the synchronization angle, the distance to fault can be calculated:

$$d_{i\_1(2)}=\operatorname{real}\left(\frac{\underline{V}_{\mathrm{A}i}\,\mathrm{e}^{\mathrm{j}\delta_{i\_1(2)}}-(\underline{V}_{\mathrm{B}i}-\underline{Z}_{i\mathrm{L}}\underline{I}_{\mathrm{B}i})}{\underline{Z}_{i\mathrm{L}}(\underline{I}_{\mathrm{A}i}\,\mathrm{e}^{\mathrm{j}\delta_{i\_1(2)}}+\underline{I}_{\mathrm{B}i})}\right) \tag{9}$$

Again, there are two solutions for the distance to fault (d_{i_1}, d_{i_2}). The solution, which is obtained for the earlier selected valid solution of the synchronization angle, is the valid solution for the distance to fault.

B. Fault location algorithm – distributed parameter line model

Applying the distributed parameter line model, the voltage at the fault point F (for the *i*-th symmetrical component), viewed from the terminals A and B, is determined as follows:

$$\underline{V}_{\mathrm{FA}i}(d,\delta)=\underline{V}_{\mathrm{FA}i}^{\mathrm{unsynchr}}\left(\cos(\delta)+\mathrm{j}\sin(\delta)\right) \tag{10}$$

$$\underline{V}_{\mathrm{FB}i}(d)=\underline{V}_{\mathrm{B}i}\cosh(\underline{\gamma}_i\ell(1-d))-\underline{Z}_{\mathrm{c}i}\underline{I}_{\mathrm{B}i}\sinh(\underline{\gamma}_i\ell(1-d)) \tag{11}$$

where:

$\underline{V}_{\mathrm{FA}i}^{\mathrm{unsynchr}}(d)=\underline{V}_{\mathrm{A}i}\cosh(\underline{\gamma}_i\ell d)-\underline{Z}_{\mathrm{c}i}\underline{I}_{\mathrm{A}i}\sinh(\underline{\gamma}_i\ell d)$,

$\underline{\gamma}_i=\sqrt{\underline{Z}'_{i\mathrm{L}}\underline{Y}'_{i\mathrm{L}}}$ – propagation constant of the line for the *i*-th symmetrical component,

$\underline{Z}_{\mathrm{c}i}=\sqrt{\underline{Z}'_{i\mathrm{L}}\big/\underline{Y}'_{i\mathrm{L}}}$ – characteristic impedance of the line for the *i*-th symmetrical component,

$\underline{Z}'_{i\mathrm{L}}=R'_{i\mathrm{L}}+\mathrm{j}\omega_1 L'_{i\mathrm{L}}$ – impedance of the line for the *i*-th symmetrical component (Ω/km),

$\underline{Y}'_{i\mathrm{L}}=G'_{i\mathrm{L}}+\mathrm{j}\omega_1 C'_{i\mathrm{L}}$ – admittance of the line for the *i*-th symmetrical component (S/km),

$R'_{i\mathrm{L}}$, $L'_{i\mathrm{L}}$, $G'_{i\mathrm{L}}$, $C'_{i\mathrm{L}}$ – resistance, inductance, conductance and capacitance of the line per km length,

ω_1 – rated angular frequency (1/s),

ℓ – length of the line (km).

Comparing (10) with (11) does not result in direct solution for the values of the synchronization angle and the distance to fault, as it was earlier for the lumped line model. This can be obtained with performing iterative calculations utilizing the Newton-Raphson method [10]. For this purpose, the following function of the sought unknowns is formulated:

$$\underline{F}_i(d,\delta)=\underline{V}_{\mathrm{FA}i}(d,\delta)-\underline{V}_{\mathrm{FB}i}(d)=0 \tag{12}$$

The iterative calculations are performed according to the following matrix formula:

$$\mathbf{X}_{\mathrm{new}}=\mathbf{X}_{\mathrm{old}}-\mathbf{J}^{-1}(\mathbf{F}_{\mathrm{old}})*\mathbf{F}_{\mathrm{old}} \tag{13}$$

where:

$$\mathbf{X}_{\mathrm{new}}=\begin{bmatrix}d_{\mathrm{new}}\\ \delta_{\mathrm{new}}\end{bmatrix},\quad \mathbf{X}_{\mathrm{old}}=\begin{bmatrix}d_{\mathrm{old}}\\ \delta_{\mathrm{old}}\end{bmatrix},\quad \mathbf{F}_{\mathrm{old}}=\begin{bmatrix}F_{\mathrm{real}}(d_{\mathrm{old}},\delta_{\mathrm{old}})\\ F_{\mathrm{imag}}(d_{\mathrm{old}},\delta_{\mathrm{old}})\end{bmatrix},$$

$$\mathbf{J}(\mathbf{F}_{\mathrm{old}})=\begin{bmatrix}\dfrac{\partial F_{\mathrm{real}}(d_{\mathrm{old}},\delta_{\mathrm{old}})}{\partial d_{\mathrm{old}}} & \dfrac{\partial F_{\mathrm{real}}(d_{\mathrm{old}},\delta_{\mathrm{old}})}{\partial \delta_{\mathrm{old}}}\\ \dfrac{\partial F_{\mathrm{imag}}(d_{\mathrm{old}},\delta_{\mathrm{old}})}{\partial d_{\mathrm{old}}} & \dfrac{\partial F_{\mathrm{imag}}(d_{\mathrm{old}},\delta_{\mathrm{old}})}{\partial \delta_{\mathrm{old}}}\end{bmatrix}.$$

The respective elements of the vector $\mathbf{F}_{\mathrm{old}}$ are defined in the following way:

$$F_{\mathrm{real}}(d_{\mathrm{old}},\delta_{\mathrm{old}})=\operatorname{real}[\underline{V}_{\mathrm{FA}i}(d_{\mathrm{old}},\delta_{\mathrm{old}})-\underline{V}_{\mathrm{FB}i}(d_{\mathrm{old}})], \tag{14}$$

$$F_{\mathrm{imag}}(d_{\mathrm{old}},\delta_{\mathrm{old}})=\operatorname{imag}[\underline{V}_{\mathrm{FA}i}(d_{\mathrm{old}},\delta_{\mathrm{old}})-\underline{V}_{\mathrm{FB}i}(d_{\mathrm{old}})]. \tag{15}$$

After taking into account (13) one obtains:

$$\begin{aligned}F_{\mathrm{real}}(d_{\mathrm{old}},\delta_{\mathrm{old}})&=\operatorname{real}[\underline{V}_{\mathrm{FA}i}^{\mathrm{unsynchr}}(d_{\mathrm{old}})]\cos(\delta_{\mathrm{old}})\\ &-\operatorname{imag}[\underline{V}_{\mathrm{FA}i}^{\mathrm{unsynchr}}(d_{\mathrm{old}}]\sin(\delta_{\mathrm{old}})-\operatorname{real}[\underline{V}_{\mathrm{FB}i}(d_{\mathrm{old}})]\end{aligned}, \tag{16}$$

$$\begin{aligned}F_{\mathrm{imag}}(d_{\mathrm{old}},\delta_{\mathrm{old}})&=\operatorname{imag}[\underline{V}_{\mathrm{FA}i}^{\mathrm{unsynchr}}(d_{\mathrm{old}})]\cos(\delta_{\mathrm{old}})\\ &+\operatorname{real}[\underline{V}_{\mathrm{FA}i}^{\mathrm{unsynchr}}(d_{\mathrm{old}})]\sin(\delta_{\mathrm{old}})-\operatorname{imag}[\underline{V}_{\mathrm{FB}i}(d_{\mathrm{old}})]\end{aligned}. \tag{17}$$

Using (16) and (17) the respective components of the Jacobian matrix $\mathbf{J}(\mathbf{F}_{\mathrm{old}})$ are determined.

The results for the synchronization angles (7) and (8) and the distance to fault (9), obtained under considering the lumped model of the line, are used as the initial values for $\delta_{\mathrm{old}}, d_{\mathrm{old}}$ in the algorithm (13). The iterative calculations are performed for the predefined fixed number of iterations or until the required convergence for the sought results is reached.

III. ATP-EMTP Based Evaluation of the Fault Location Algorithm

The presented fault location algorithm has been evaluated with using the fault data obtained from ATP-EMTP [11] versatile simulations of faults in the power network containing the 400 kV, 300 km transmission line (Table I). In order to show the errors of the presented method itself, the CTs and VTs have been intentionally modeled as errorless transforming devices. The secondary signals of such idealized instrument transformers are passed via second order analog anti-aliasing filters with the cut-off frequency set to 350 Hz. Then, the signals are sampled at 1000 Hz and the full-cycle Fourier orthogonal filters were applied for determining their phasors. Different specifications of faults have been considered. The evaluation results presented in the paper, concern the most frequent single phase to ground faults (a-g).

TABLE I. PARAMETERS OF THE 400 KV TRANSMISSION NETWORK

Component:	Parameter:	
Line AB	ℓ	300 km
	$\underline{Z}'_{1L}$	(0.0276+j0.3151) Ω/km
	$\underline{Z}'_{0L}$	(0.2750+j1.0265) Ω/km
	C'_{1L}	13.0 nF/km
	C'_{0L}	8.5 nF/km
Equivalent system at terminal A	$\underline{Z}_{1SA}$	(1.312+j15.0) Ω
	$\underline{Z}_{0SA}$	(2.334+j26.6) Ω
	Angle of EMF from phase 'a'	0^o
Equivalent system at terminal B	$\underline{Z}_{1SB}$	$2\,\underline{Z}_{1SA}$
	$\underline{Z}_{0SB}$	$2\,\underline{Z}_{0SA}$
	Angle of EMF from phase 'a'	30^o

A. Fault location example

In Fig. 3 to Fig. 5, the example of fault location is presented. The specifications of the fault – a-g fault, distance to fault: d=0.8 p.u., fault resistance: R_F=10 Ω, actual synchronization angle: δ=36^o (obtained by introducing a delay of signals from the side A by 2 samples).

The continuous values results for the synchronization angle (Fig. 4) and distance to fault (Fig. 5) are singled by averaging (subscript: av.) within the interval (from 30 to 50) ms after the fault inception.

Using positive sequence quantities the following averaged values of the synchronization angle have been obtained: 94.28^O, 37.42^O, while using the negative sequence components: 36.11^O, -143.78^O (Fig. 4). Among all four possible pairs of the calculated results: (94.28^O, 36.11^O), (94.28^O, -143.78^O), (37.42^O, 36.11^O), (37.42^O, -143.78^O) only one pair (37.42^O, 36.11^O) consists of the synchronization angle results, which is close to each other and do not differ much. Such pair with coincident results indicates the valid solution for the synchronization angle. Taking these values: 37.42^O – for the positive sequence and 36.11^O – for the negative sequence, respectively, the distance to fault (Fig. 5) is determined. In case of using the positive sequence quantities:

- for the lumped line model: 0.8964 p.u.
- for the distributed parameter line model: 0.8003 p.u.

Applying the negative sequence components as the fault locator input signals, the following results have been obtained:

- for the lumped line model: 0.7948 p.u.
- for the distributed parameter line model: 0.7998 p.u.

B. Evaluation of the algorithm for a-g faults

In Tables II and III the results for the a-g faults, applied through R_F=10 Ω fault resistance at different locations (d = 0.1 to 0.9 p.u.), have been gathered. The signals obtained from ATP-EMTP simulations are in natural way perfectly synchronized. In order to show performance of the presented algorithm the voltage and current signals measured at the terminal A are delayed by 18^o (it corresponds to the single sampling interval for 50 Hz signals digitalized at 1000 Hz).

Processing the positive sequence quantities with the lumped transmission line model (iteration '0') results in errors reaching: 1.98^O – for the synchronization error (Table II) and 0.069 (p.u.) – for the distance to fault (Table III). Applying the results of the iteration '0' as the starting data to the Newton-Raphson calculations (with use of the distributed parameter line model), already in the first iteration (iteration '1') considerable improvement of accuracy is achieved. Practically, due to very fast convergence, it is sufficient to perform only a single iteration of the calculations.

TABLE II. DETERMINATION OF THE SYNCHRONIZATION ANGLE WITH USE OF POSITIVE SEQUENCE QUANTITIES (A-G FAULT, R_F=10 Ω, δ_{ACTUAL}=18^O)

Actual distance d (p.u.)	Calculated synchronization angle: δ(^{o}) in particular 'iterations'			
	'0'	'1'	'2'	'3'
0.1	17.1444	17.9964	18.0349	18.0349
0.2	17.4581	18.0090	18.0254	18.0254
0.3	17.6844	18.0071	18.0127	18.0127
0.4	17.9322	18.0040	18.0046	18.0046
0.5	18.2298	17.9963	17.9962	17.9962
0.6	18.5834	17.9826	17.9851	17.9851
0.7	18.9955	17.9678	17.9745	17.9745
0.8	19.4552	17.9435	17.9536	17.9536
0.9	19.9766	17.9089	17.9185	17.9185

TABLE III. DETERMINATION OF THE DISTANCE TO FAULT WITH USE OF POSITIVE SEQUENCE QUANTITIES (A-G FAULT, R_F=10 Ω, δ_{ACTUAL}=18^O)

Actual distance d (p.u.)	Calculated distance to fault: d (p.u.) in particular 'iterations'			
	'0'	'1'	'2'	'3'
0.1	0.0458	0.1002	0.1000	0.1000
0.2	0.1455	0.1999	0.1997	0.1997
0.3	0.2558	0.2994	0.2993	0.2993
0.4	0.3747	0.3991	0.3990	0.3990
0.5	0.4989	0.4988	0.4988	0.4988
0.6	0.6244	0.5989	0.5986	0.5986
0.7	0.7467	0.6991	0.6984	0.6984
0.8	0.8624	0.7996	0.7983	0.7983
0.9	0.9690	0.9002	0.8984	0.8984

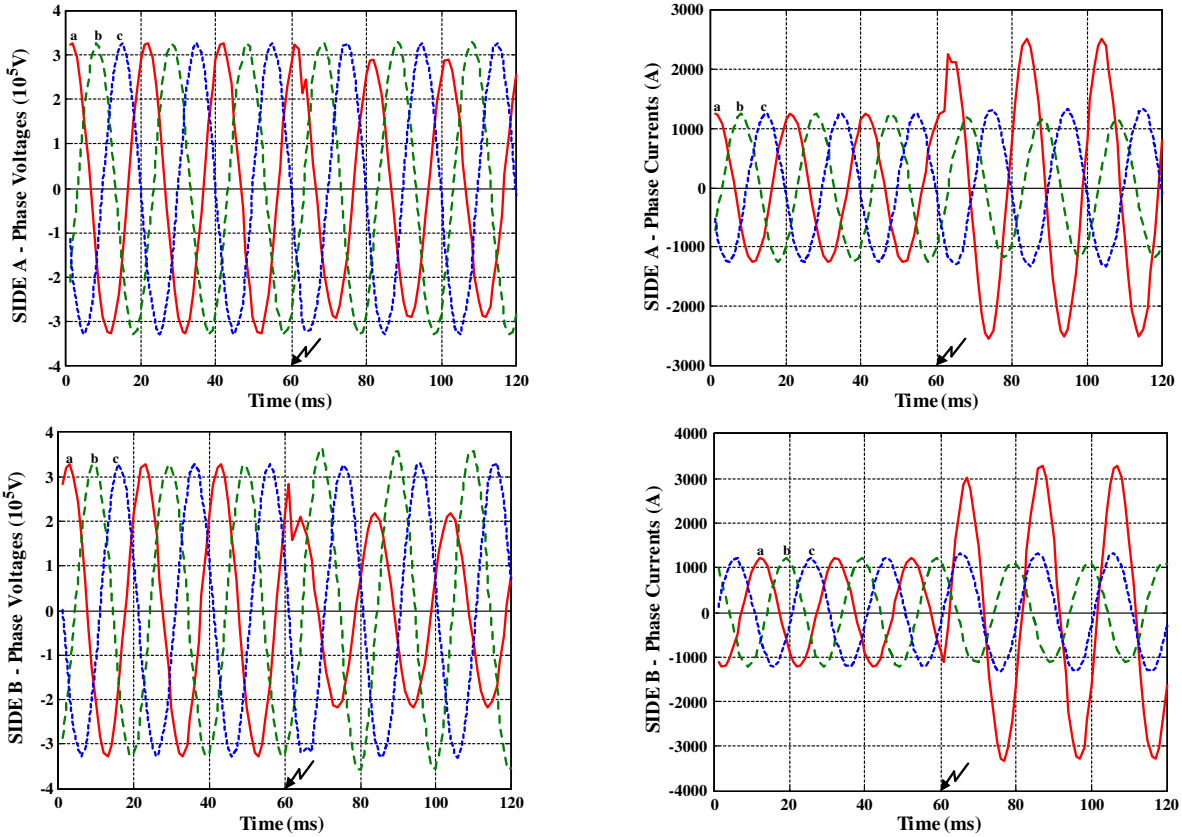

Fig. 3. The example – input signals of the fault location algorithm.

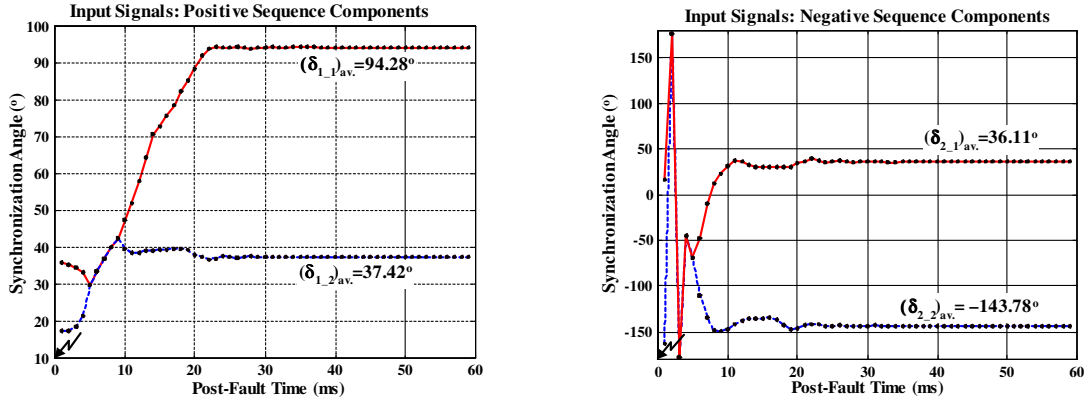

Fig. 4. The example – calculated values of the synchronization angle with use of the positive and negative sequence components.

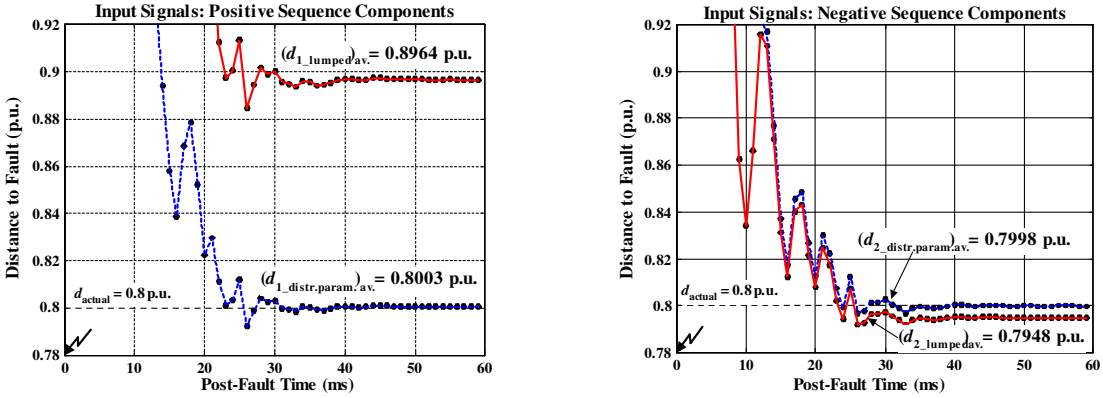

Fig. 5. The example – calculated distance to fault applying the lumped and distributed parameter line models, with use of the positive and negative sequence components.

IV. New Contribution

This paper is a continuation of [10], where the two-end unsynchronized fault location method has been introduced. It is important that in case of such measurements there is a need for phase alignment, as explained in Fig. 2. In this paper, formulae for the synchronization angles (7) and (8) together with remarks useful for implementing the algorithm into the Matlab program, are also added.

It is shown (the example presented in Fig. 3–Fig. 5) that the selection of the valid result, can also be performed by analyzing the solutions for the synchronization angle. This is considered as an alternative to the approach from [10].

ATP-EMTP evaluation results, which are gathered in Fig.3 - Fig.5, together with the results presented in [10], show the robustness of the algorithm against a change of direction of the pre-fault power flow. It has not experienced even a single case, where the convergence is not met. Fast convergence is due to the fact that , starting calculations from the values calculated for the lumped parameter line model, does not differ much from the final values (for the distributed parameter line model). It has been shown that, in practice, it is sufficient to perform only a single iteration, which in fact leads to an algorithm of non-iterative feature. After performing three iterations, the distance to fault results do not change more than 0.01%.

V. Conclusions

The presented two-end unsynchronized fault location algorithm is formulated in terms of phasors of the symmetrical components and consists of the two calculation stages.

In the first stage the simple lumped model of a transmission line, without accounting for the shunt capacitances effect, is utilized. The results from this stage are then used as the starting values for the Newton-Raphson iterative calculations (second stage). As a result of strict consideration of the distributed parameter line model, the unknown synchronization angle is determined precisely, and, therefore, accuracy of the presented fault location algorithm can be considered as comparable to the ensured by the methods based on two-end synchronized measurements.

The performed testing and evaluation with the fault data obtained from ATP-EMTP simulations proved satisfactory performance and high accuracy of the presented fault location algorithm.

VI. References

[1] L. Eriksson, M. M. Saha and G. D. Rockefeller, "An accurate fault locator with compensation for apparent reactance in the fault resistance resulting from remote-end infeed", *IEEE Trans. Power Apparatus and Systems*, Vol. PAS–104, pp. 424–436, February 1985.

[2] T. Kawady and J. Stenzel, "A practical fault location approach for double circuit transmission lines using single end data", *IEEE Trans. Power Delivery*, Vol. 18, pp. 1166-1173, April 2003.

[3] P. A. Crossley and E. Southern, "The impact of the global positioning system (GPS) on protection & control", in *Proc. 1998 the 11th International Conference on Power System Protection – PSP '98*, Bled, Slovenia, pp. 1–5.

[4] R. K. Aggarwal, D. V. Coury, A. T. Johns and A. Kalam, "A practical approach to accurate fault location on extra high voltage teed feeders", *IEEE Trans. Power Delivery*, Vol. 8, pp. 874-883, July 1993.

[5] M. Kezunovic and B. Perunicic, "Automated transmission line fault analysis using synchronized sampling at two ends", *IEEE Trans. Power Systems*, Vol. PS–11 (1), pp. 441–447, February 1996.

[6] D. Novosel, D. G. Hart, E. Udren and J. Garitty, "Unsynchronized two-terminal fault location estimation", *IEEE Trans. Power Delivery*, Vol. 11, pp. 130–138, January 1996.

[7] M. S. Sachdev and R. Agarwal, "A technique for estimating line fault locations from digital distance relay measurements", *IEEE Trans. on Power Delivery*, Vol. PWRD–3, pp. 121–129, January 1988.

[8] J. Izykowski, E. Rosolowski and M. M. Saha, "Postfault analysis of operation of distance protective relays of power transmission lines", *IEEE Trans. Power Delivery*, Vol. 22, pp. 74-81, January 2007.

[9] I. Zamora, J. F. Minambres, A. J. Mazon, R. Alvarez-Isasi and J. Lazaro, "Fault location on two-terminal transmission lines based on voltages", *IEE Proceedings – Gener. Transm. Distrib.,* Vol. 143, pp. 1–6, January 1996.

[10] J. Izykowski, R. Molag, E. Rosolowski and M. M. Saha, "Accurate location of faults on power transmission lines with use of two-end unsynchronized measurements" *IEEE Trans. Power Delivery*, VOL. 21, pp. 627-633, April 2006.

[11] H. W. Dommel, *Electro-Magnetic Transients Program*, BPA, Portland, Oregon, 1986.

[12] MATLAB, *High-Performance Numeric Computation and Visualization Software. External Interface Guide*, The Mathworks, Inc., January 1993.

VII. Biographies

Murari Mohan Saha (M´76, SM´87) was born in 1947 in Bangladesh. He received B.Sc.E.E. and M.Sc.E.E. from Bangladesh University of Engineering and Technology (BUET), Dhaka in 1968 and 1970. respectively. In 1972, he completed M.S.E.E. and in 1975 he was awarded with Ph.D. from the Technical University of Warsaw, Poland. He joined ASEA, Sweden, in 1975. Currently he is a Senior Research and Development Engineer at ABB Power Technologies, Västerås, Sweden. His areas of interest are measuring transformers, and protective relays.

Jan Izykowski (M'97, SM'04) was born in 1949 in Poland. He received his M.Sc., Ph.D. and D.Sc. degrees from the Faculty of Electrical Engineering of Wroclaw University of Technology (WUT) in 1973, 1976 and in 2001, respectively. In 1973 he joined Institute of Electrical Engineering of the WUT. Presently he is an Associate Professor. His research interests are in power system transients simulation, power system protection and control, and fault location.

Eugeniusz Rosolowski (M'1997, SM'00) was born in 1947 in Poland. He received his M.Sc. degree in Electrical Eng. from the Wroclaw University of Technology (WUT) in 1972. From 1974 to 1977, he studied in Kiev Politechnical Institute, where he received Ph.D. in 1978. In 1993 he received D.Sc. from the WUT, where presently he is a Professor. His research interests are in power system analysis and microprocessor applications in power systems.

Rafal Molag was born in Poland in 1977. He received his M.Sc. degree from the Faculty of Electrical Engineering of Wroclaw University of Technology (WUT) in 2002. He is currently pursuing the Ph.D. degree in electrical engineering at Institute of Electrical Power Engineering of WUT. His research interests are in power system protection, and fault location.